analytical chemistry

ARTICLE

pubs.acs.org/ac

Ultrasensitive Immunoassay of Protein Biomarker Based on Electrochemiluminescent Quenching of Quantum Dots by Hemin Bio-Bar-Coded Nanoparticle Tags

Dajie Lin,[†] Jie Wu,[†] Feng Yan,[‡] Shengyuan Deng,[†] and Huangxian Ju*[,†]

[†]State Key Laboratory of Analytical Chemistry for Life Science, Department of Chemistry, Nanjing University, Nanjing 210093, P. R. China

[‡]Jiangsu Institute of Cancer Prevention and Cure, Nanjing 210009, P. R. China

ABSTRACT: A hemin bio-bar-coded nanoparticle probe labeled antibody was designed by the assembly of antibody and alkylthiol-capped bar-code G-quadruplex DNA on gold nanoparticles and the interaction of hemin with the DNA to form a G-quadruplex/hemin bio-bar-code. An ultrasensitive immunoassay method was developed by combining the labeled antibody with an electrochemiluminescent (ECL) immunosensor for protein. The ECL immunosensor was constructed by a layer-by-layer modification of carbon nanotubes, CdS quantum dots (QDs), and capture antibody on a glassy carbon electrode. In air-saturated pH 8.0 PBS the immunosensor showed a carbon-nanotube-enhanced cathodic ECL emission of QDs. Upon the formation of immunocomplex, the ECL intensity decreased owing to the consumption of ECL coreactant in bio-bar-code electrocatalyzed reduction of dissolved oxygen. Using α-fetoprotein as model analyte, the quenched ECL could be used for immunoassay with a linear range of 0.01 pg mL^{-1} to 1 ng mL^{-1} and a detection limit of 1.0 fg mL^{-1}. The wide detection range and high sensitivity resulted from the enhanced ECL emission and highly efficient catalysis of the bio-bar-code. The immunosensor exhibited good stability and acceptable fabrication reproducibility and accuracy, showing great promise for clinical application.

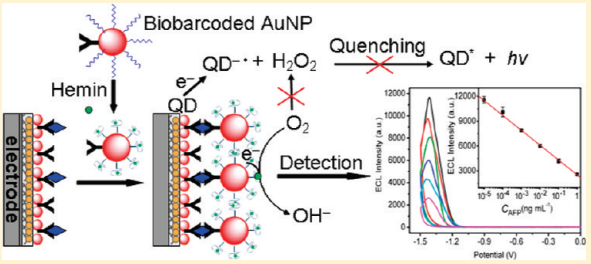

Highly sensitive and selective determination of protein biomarkers is critical to many areas, such as disease diagnosis, biomedical research, and biodefense applications.[1−3] Recently, great efforts have been made to develop ultrasensitive immunosensors for the detection of low-abundance biomarkers. Signal amplification is the most popular strategy that has been employed for the development of ultrasensitive immunoassay methods. Most of the signal amplification methods employ multienzyme report probes, which are prepared by bioconjugating large amounts of enzymes, including alkaline phosphatase,[4,5] horseradish peroxidase (HRP),[6−9] and glucose oxidase,[10] on nanocarriers, such as nanoparticles,[6−8] carbon nanotubes (CNTs),[4,5,10] and magnetic beads,[9] to enhance the enzymatically catalytic signal. However, the practical applications of these report probes are limited due to the denaturation and leakage of enzymes[11] and the time-consuming and costly preparation and purification process of enzymes.[12,13]

Artificial mimic enzymes, especially DNAzymes, recently intrigued researchers as catalytic amplifiers in biosensing events.[14−17] Compared with protein enzymes, the DNAzymes are more stable and relatively less expensive to produce by the polymerase chain reaction. Moreover, the DNAzymes can be denatured and renatured many times without losing activity. G-quadruplex-based DNAzyme is an interesting DNAzyme with peroxidase-like activities, in which the G-quadruplex structure can be formed by the conjugation between a single-stranded guanine-rich nucleic acid and hemin.[16,17] Such DNAzyme can catalyze the reduction of H_2O_2 or dissolved oxygen by some redox-active reagents and has been extensively used as a catalytic amplifier to construct biosensors. For example, Willner's group used it as a label to sensitively detect DNA hybridization and proteins.[15,16] This work developed a new bio-bar-coded nanoparticle probe for bio-bar-code assay by the assembly of antibody (Ab_2) and alkylthiol-capped bar-code G-quadruplex DNA on gold nanoparticle (AuNP) and the interaction of hemin with the DNA.

The bio-bar-code assay based on oligonucleotide-functonalized AuNPs has been reported by scanometric detection with universal probe.[3,18] This method has the advantages in terms of sensitivity and selectivity over other biodetection schemes using conventional probes. For example, the detection limits for protein targets can be 4−6 orders of magnitude lower than that from ELISAs[3] due to the loading of DNA on the unit area of AuNP, which is at least 5 times higher[19] than the loading of 11 HRP molecules on AuNP with 13-nm diameter.[20] On the basis of this strategy a bio-bar-code assay method for DNA has been developed by using tris(2,2′-bipyridyl)ruthenium-labeled bar-code DNA to produce electrochemiluminescent (ECL) emission.[21]

Received: February 15, 2011
Accepted: May 21, 2011
Published: May 22, 2011

Scheme 1. Schematic Representation of (A) Preparation Procedure of Ab_2−Bio-Bar-Coded AuNP−G-Quadruplex/Hemin Probe, and (B) Immunosensor Preparation and Sandwich-Type Detection Procedure

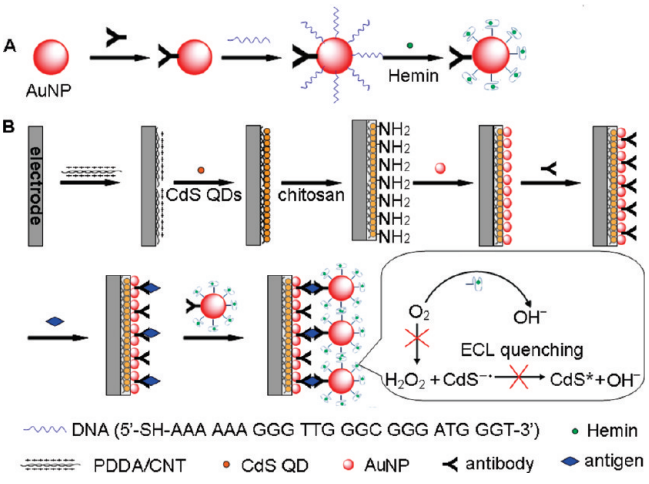

This work combined the ECL emission of QDs with bio-bar-code assay technology using an Ab_2−bio-bar-coded AuNP probe to develop a novel bio-bar-code method for ultrasensitive immunoassay of target protein, in which the signal recognition event could be amplified to form the enormous G-quadruplex DNA for following measurement. Compared to early bio-bar-code assay methods for protein detection,[3,18] the proposed method did not need other time-consuming detection procedures such as the release and collection of bar-code DNA from the bio-bar-code probe and the hybridization of bar-code DNA to produce detection signal.

It is well-known that semiconductor QDs have been widely used in bioanalysis[22−25] due to their controllable size and emission wavelength, high photoluminescence (PL) yield, and good chemical stability.[26,27] The immunosensing based on the ECL emission of QDs has attracted increasing concern.[28−30] The developed ECL immunosensing methods mainly include two mechanisms: steric hindrance produced from the formation of immunocomplex[28,29] and consumption of ECL coreactant in an enzymatic reaction.[30] These effects lead to target-concentration-dependent decrease of ECL emission. This work made use of the high loading of hemin bio-bar-code as a highly efficient peroxidase-like active DNAzyme to design a signal amplification strategy. By combining the sensitizing effect of CNTs to the ECL emission of QDs on an immunosensor surface[31] with the attached hemin bio-bar-code to amplify the quenching of ECL by an enzymatic reaction, an ultrasensitive ECL immunoassay method for protein biomarker was developed.

Herein, the ECL immunosensor was constructed by immobilizing CdS QDs and capture antibody on a poly(diallyldimethylammonium chloride)-functionalized CNTs-modified (PDDA/CNTs) electrode (Scheme 1). With a sandwich immunoassay, the bio-bar-coded probe was captured on the immunosensor surface to catalyze the reduction of dissolved oxygen, the coreactant for cathodic ECL emission, leading to a decrease of ECL intensity. The high loading of hemin bio-bar-code for signal recognition event and the strong catalytic activity of the hemin bio-bar-code for quenching the ECL emission led to ultrahigh sensitivity. The proposed immunoassay method could detect protein in a concentration range of 5 orders of magnitude with a detection limit down to femtograms/milliliter level that was 4 orders of magnitude lower than that using QD ECL.[30] Moreover, this method avoided the need of deoxygenation for electrochemical immunoassay and hydroquinone to consume the self-produced coreactant[30] and thus provided a promising potential in clinical diagnosis, especially in point-of-care testing.

EXPERIMENTAL SECTION

Materials and Reagents. Mouse monoclonal anti-α-fetoprotein antibodies (anti-AFP, clone no. A14C11 and A46C9 as the capture and the secondary antibodies, respectively) were purchased from Shuangliu Zhenglong Biochem. Lab (Chengdu, China). AFP standard solutions with concentrations from 0 to 1 ng mL^{-1} were from ELISA kits of AFP, which were supplied by Fujirebio Diagnostics AB (Göteborg, Sweden). The synthetic oligonucleotide was purchased from Shanghai Sangon Biological Engineering Technology & Services Co. Ltd. Its base sequence is 5′-SH-AAA AAA GGG TTG GGC GGG ATG GGT-3′. Poly(diallyldimethylammonium chloride) (PDDA, 20%, w/w in water, MW 200 000−350 000), hemin, mercaptopropionic acid (MPA), bovine serum albumin (BSA), and chitosan (≥85% deacetylation) were obtained from Sigma-Aldrich Chemical Co. (St. Louis, MO). Cadmium chloride ($CdCl_2 \cdot 2.5H_2O$) was purchased from Alfa Aesar China Ltd. Multiwalled carbon nanotubes (CNTs, CVD method, purity ≥98%, diameter 10−20 nm, and length 5−15 μm) were purchased from Nanoport Co. Ltd. (Shenzhen, China). Chloroauric acid ($HAuCl_4 \cdot 4H_2O$) and trisodium citrate were obtained from Shanghai Reagent Co. (Shanghai, China). Ultrapure water obtained from a Millipore water purification system (≥18 MΩ, Milli-Q, Millipore) was used in all assays. Phosphate-buffered saline (PBS, 0.02 M) of various pHs was prepared by mixing the stock solutions of NaH_2PO_4 and Na_2HPO_4. The washing buffer was PBS (0.02 M, pH 7.4) containing 0.05% (w/v) Tween-20 (PBST). The clinical serum samples were from Jiangsu Institute of Cancer Prevention and Cure. All other reagents were of analytical grade and used as received.

CNTs were first sonicated with 3:1 (v/v) H_2SO_4/HNO_3 for 4 h to obtain carboxylic group-functionalized CNTs. The resulting dispersion was filtered and washed repeatedly with water until the pH was about 7.0. The oxidized CNTs were further functionalized with PDDA according to the reported method.[10] The collected PDDA-functionalized CNTs (PDDA/CNTs) were redispersed in water to a concentration of 1.0 mg mL^{-1}.

Preparation of Ab_2−Bio-Bar-Coded AuNP−G-Quadruplex/Hemin Probe. First, the colloidal AuNPs with 13-nm diameter were prepared according to the previous protocol.[10] Briefly, 100 mL of 0.01% $HAuCl_4$ solution was boiled with vigorous stirring, and 2.5 mL of 1% trisodium citrate solution was quickly added to the boiling solution. The solution turned deep red, indicating the formation of AuNPs. Followed by continued stirring and cooling down, the resulting Au colloidal solution was stored in brown glass bottles at 4 °C before use.

The bio-bar-coded nanoparticle probe was prepared according to a previous report with slight modification.[18] As shown in Scheme 1A, after adjusting the pH of 3 mL of 4 nM Au colloidal solution to 9.2, 9 μL of 1.3 mg mL^{-1} anti-AFP antibody (Ab_2) was added to the solution, followed by an incubation at 4 °C for 4 h with slow stirring. The resulting Ab_2-attached AuNPs were reacted with 1 OD alkylthiol-capped bar-code G-quadruplex DNA for 16 h, followed by a salt-stabilization in 0.1 M NaCl.

dx.doi.org/10.1021/ac200398x |Anal. Chem. 2011, 83, 5214–5221

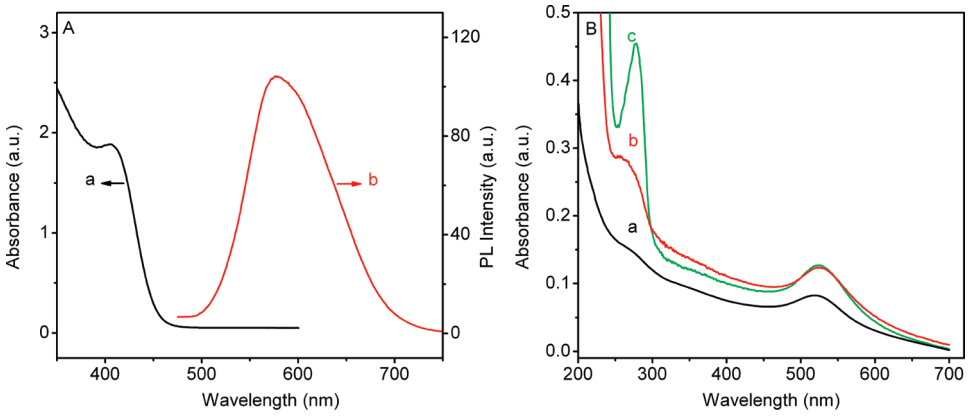

Figure 1. (A) UV−vis (a) and PL (λ_{ex} = 449 nm) (b) spectra of the as-prepared CdS QDs, and (B) UV−vis spectra of AuNPs (a), Ab_2-attached AuNPs (b) and Ab_2−bio-bar-coded AuNP−G-quadruplex/hemin probe (c) in 10 mM pH 7.4 PBS.

Afterward, 0.3 mL of blocking buffer (10 mM PBS containing 0.1 M KCl, 0.02% Tween-20 and 10% BSA, pH 7.4) was dropped into the solution, and the mixture was stirred at 4 °C for 2 h. A 0.3 mL portion of 5 μM hemin was then added to the resulting solution. After stirring for 6 h, the excess of antibody, DNA, and hemin were removed by centrifugation (12 000 rpm, 30 min at 4 °C) and redispersed in 10 mM PBS containing 0.1 M KCl, which was repeated for further purification. The obtained hemin bio-bar-coded nanoparticle probe was redispersed in 2 mL of 0.01 M pH 7.4 PBS containing 0.1 M KCl and stored at 4 °C.

Preparation of ECL Immunosensor. The water-soluble CdS QDs were prepared using MPA as stabilizing agent according to a method similar to that reported previously.[32] Briefly, 86 μL of MPA was added to 20 mL of 20 mM $CdCl_2$ solution. After adjusting the pH to 10, 20 mL of 20 mM thioacetamide aqueous solution was added with extensive stirring for 30 min. After refluxing at 80 °C for 10 h, the formed CdS colloid was dialyzed exhaustively against water overnight at room temperature to obtain CdS QDs solution. The product was condensed by ultrafiltration at 10 000 rpm for 10 min, and the upper phase was decanted and kept at 4 °C.

A glassy carbon electrode (GCE) with 3-mm diameter was polished to a mirror using 1.0, 0.3, and 0.05 μm alumina slurry (Beuhler) followed by rinsing thoroughly with deionized water. After successive sonication in 1:1 nitric acid, acetone and deionized water, the electrode was rinsed with water and allowed to dry at room temperature. As shown in Scheme 1B, 5 μL of 1.0 mg mL^{-1} PDDA/CNTs solution was dropped on the pretreated GCE. After drying in air, 5 μL of 10 μM MPA-CdS QDs was dropped on the PDDA/CNTs film and dried in air again. Three microliters of 0.05% chitosan solution was then coated on the film. After activating the chitosan film with 5 μL of Au colloidal solution at room temperature for 4 h, 5 μL of 0.1 mg mL^{-1} anti-AFP antibody (Ab_1) was coated on the electrode by an overnight incubation at 4 °C. Subsequently, the resulting electrode was washed three times with PBST and PBS to remove the physically absorbed Ab_1 and blocked with 5 μL of 5% BSA solution for 1 h at room temperature to form the ECL immunosensor.

Apparatus and Measurement Procedure. The electrochemical and ECL measurements were carried out on an MPI-E multifunctional electrochemical and chemiluminescent analytical system (Xi'an Remex Analytical Instrument Ltd. Co.) at room temperature with a configuration consisting of a GCE (3 mm in diameter) as working, a platinum wire as counter, and Ag/AgCl (saturated KCl solution) as reference electrodes. The ECL emission window was placed in front of the photomultipier tube (PMT, detection range from 300 to 650 nm) biased at 900 V. The PL experiment was performed on a RF-5301 PC fluorometer (Shimadzu Co.). The UV−vis absorption spectrum was observed with a UV-3600 UV−vis spectrophotometer (Shimadzu). Electrochemical impedance spectroscopic (EIS) analysis was performed with an Autolab PGSTAT12 (Ecochemie) in 0.1 M KCl containing 5 mM $Fe(CN)_6]/K_3[Fe(CN)_6]$. Scanning electron micrographs (SEM) were obtained with a Hitachi S-3000N scanning electron microscope at an acceleration voltage of 10 kV.

To carry out the immunoreaction and ECL measurement, the immunosensor was first incubated with 5 μL of the AFP standard solution or serum sample with certain concentration for 30 min at room temperature. After washing with PBST and PBS, the immunosensor was further incubated with 5 μL of Ab_2−bio-bar-coded AuNP−G-quadruplex/hemin probe for 30 min at room temperature, followed by washing with PBST and PBS. Finally, the ECL signal was detected in 0.1 M pH 8.0 PBS containing 0.1 M KCl. The reference levels of AFP in the human serum samples were detected with an automation electrochemiluminescent analyzer (Elecsys 2010, Roche).

RESULTS AND DISCUSSION

Characterization of CdS QDs. UV−vis and PL spectra were used to characterize the formation of CdS QDs. The UV−vis spectrum of the as-prepared CdS QDs showed a clear absorption at 405 nm (Figure 1A, curve a), from which the size of the resulting CdS QDs and concentration of QDs solution could be estimated to be 3.7 nm and 4.27 μM from the absorption peak and Peng's empirical equations.[33] The PL spectrum (excited at 449 nm) of the CdS QDs solution showed a strong emission peak with a maximum intensity at 577 nm (Figure 1A, curve b). The similar PL excited wavelength and absorption wavelength indicated the emitter was the excited state of QD core (QD*).[32]

Characterization of Ab_2-Bio-Bar-Coded AuNP−G-Quadruplex/Hemin Probe. The UV−vis spectra of AuNPs, Ab_2-attached AuNPs, and Ab_2−bio-bar-coded AuNP−G-quadruplex/hemin probe are shown in Figure 1B. The size of the AuNPs could be estimated to be 13 nm from the absorption peak at 519 nm (curve a), which was further confirmed by TEM (data not shown here). After the Ab_2 molecules were attached to the

dx.doi.org/10.1021/ac200398x |*Anal. Chem.* 2011, 83, 5214–5221

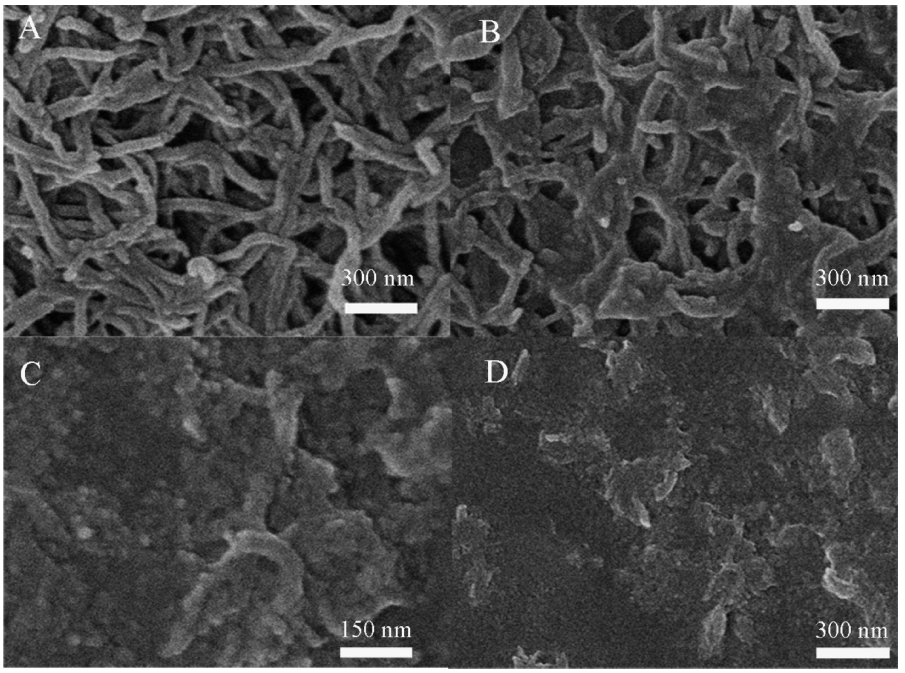

Figure 2. SEM images of PDDA/CNTs (a), QDs/PDDA/CNTs (b), AuNPs/chitosan/QDs/PDDA/CNTs (c), and Ab_1/AuNPs/chitosan/QDs/PDDA/CNTs (d).

surface of AuNPs, the absorption peak of AuNPs slightly red-shifted (around 523 nm), while a 270 nm absorption peak appeared (curve b), which was corresponding to the typical protein absorption peak, indicating the successful loading of Ab_2. Compared with the absorption peak of Ab_2-attached AuNPs, a strong absorption at approximately 270 nm appeared for Ab_2−bio-bar-coded AuNP−G-quadruplex/hemin probe (curve c), demonstrating the successful modification of G-quadruplex oligonucleotides on the AuNPs. The average surface coverage of the oligonucleotide on one probe was calculated to be 50, obtained by determining spectroscopically the amount of nontagged oligonucleotide, which was coincident to the loading of DNA on the unit area of AuNP reported previously.[21]

Characterization of Immunosensor. The SEM image of PDDA/CNTs film displayed a well-dispersed structure in the form of small bundles or single tubes with diameters of 30−40 nm (Figure 2A). After CdS QDs were assembled on the PDDA/CNTs, a denser homogeneous structure could be observed (Figure 2B), indicating the attachment of QDs on PDDA/CNTs film through electrostatic adsorption. After chitosan and AuNPs were coated on the QDs/PDDA/CNTs/GCE in sequence, the surface showed a smoother and more uniform three-dimensional porous structure (Figure 2C). Upon the immobilization of Ab_1, an obvious aggregation of the trapped biomolecules with a regular distribution could be observed on the surface (Figure 2D), indicating the successful assembly of the capture antibody on the immunosensor surface through the AuNPs.

As shown in Figure 3A, the bare GCE showed a relatively small electron-transfer resistance, R_{et} (curve a). After PDDA/CNTs and chitosan film was formed on the electrode, a smaller R_{et} was observed (curve b), while the QDs and chitosan film showed a much larger R_{et} (curve c). The presence of CNTs in QDs and chitosan film could greatly decrease the R_{et} (curve d). These results indicated that the high electrical conductivity of CNTs could lower the impendance of the film and facilitate the electron transfer between the electrode and the surface-coated QDs. As the Ab_1, BSA, antigen, Ab_2, HRP-labeled Ab_2, and probe-labeled Ab_2 could all resist the electron transfer kinetics of redox probe at the electrode interface, an increase tendency of the impedance was observed during their stepwise attachment (Figure 3B, curves a−g), which testified to the immobilization of these substances on the electrode surface. It was noted that the impedances of the immunosensor surfaces with and without hemin were similar (Figure 3B, curves g and f), indicating that the binding of hemin did not affect the electron transfer and the diffusion of redox species.

ECL Emission of Immunosensor. The chitosan/QDs/GCE showed a cathodic ECL emission in air-saturated pH 8.0 PBS, with an emission peak at −1.4 V (Figure 4A, curve a). In order to obtain higher sensitivity, CNTs were used to enhance the ECL emission by reducing the injection barrier of electrons to QDs.[32,34] However, as shown in curve b, Figure 4A, in the presence of carbon nanotubes the ECL intensity did not increase, though it occurred at a relatively low potential of −1.2 V due to the high electrical conductivity of CNTs. This was caused by the blackbody effect.[34] Thus, PDDA was used to functionalize CNTs for improving the dispersion of CNTs and the attachment of QDs on CNTs, which decreased the blackbody effect. As expected, a 5-fold higher ECL intensity than that from chitosan/QDs/CNTs was observed at chitosan/QDs/PDDA/CNTs modified GCE (Figure 4A, curve c). According to the literature,[30,34] the ECL processes in air-saturated solution could be expressed as follows:

$$\text{CdS QD} + e^- \rightarrow \text{CdS QD}^{-\bullet} \quad (1)$$

$$O_2 + 2e^- + 2H_2O \rightarrow H_2O_2 + 2OH^- \quad (2)$$

$$2\text{CdS QD}^{-\bullet} + H_2O_2 \rightarrow 2OH^- + 2\text{CdS QD}^{*} \quad (3)$$

dx.doi.org/10.1021/ac200398x |*Anal. Chem.* 2011, 83, 5214–5221

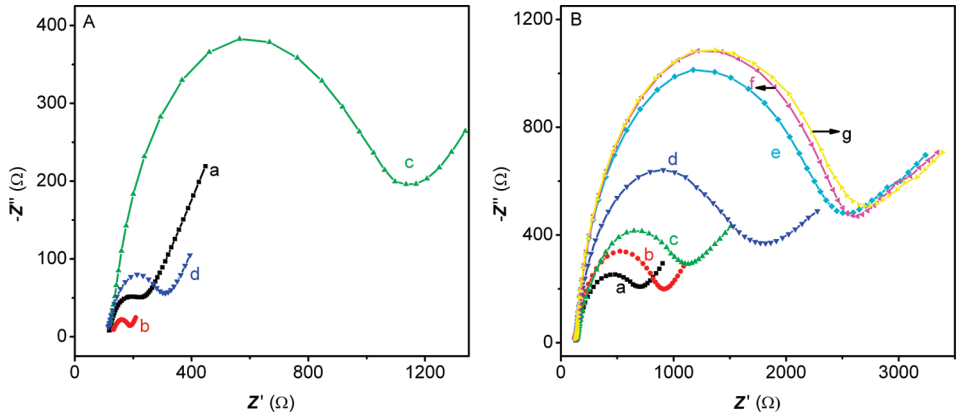

Figure 3. EIS of (A) bare GCE (a), chitosan/PDDA/CNTs/GCE (b), chitosan/QDs/GCE (c), and chitosan/QDs/PDDA/CNTs/GCE (d) and (B) Ab_1/chitosan/QDs/PDDA/CNTs/GCE before (a) and after (b) blocking with BSA, BSA blocked Ab_1/chitosan/QDs/PDDA/CNTs/GCE incubated with 1 ng mL^{-1} AFP (c), c incubated with Ab_2 (d), c incubated with HRP−Ab_2 double-codified AuNPs (e), and c incubated with Ab_2−bio-bar-coded AuNPs without (f) and with (g) hemin in 0.1 M KCl containing 5 mM $Fe(CN)_6^{2-/3-}$.

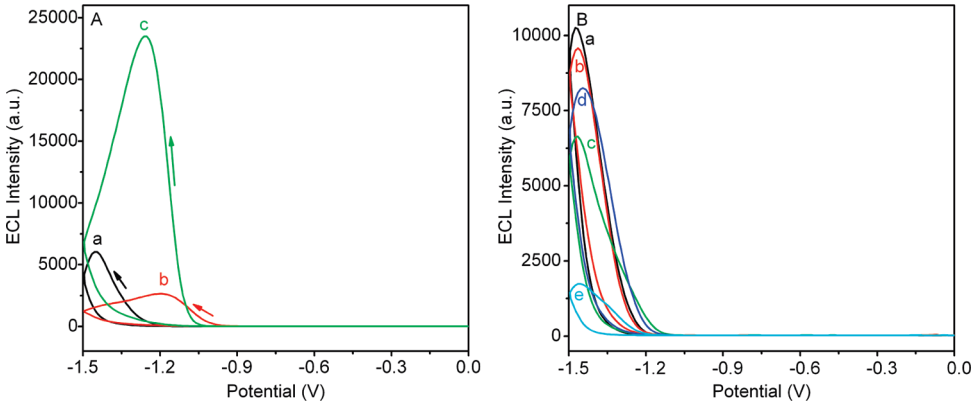

Figure 4. ECL potential curves of (A) chitosan/QDs/GCE (a), chitosan/QDs/CNTs/GCE (b), and chitosan/QDs/PDDA/CNTs/GCE (c) and (B) Ab_1/chitosan/QDs/PDDA/CNT/GCE after a sandwich immunoreaction with 1 ng mL^{-1} AFP and 0 μg mL^{-1} Ab_2 (a), 1 μg mL^{-1} Ab_2 (b), HRP−Ab_2 double-coated AuNPs (c), and Ab_2−bio-bar-coded AuNPs without (d) and with (e) hemin.

$$CdS\ QD^{*} \rightarrow CdS\ QD + h\nu \qquad (4)$$

Because chitosan has an abundance of amino groups, it was used to attach AuNPs for assembly of antibody. The resulting immunosensor showed twice lower ECL emission than the chitosan/QDs/PDDA/CNTs modified GCE, while the formation of immunocomplex with antigen made the ECL emission further decrease (Figure 4B, curve a) due to the change of electron-transfer resistance (Figure 3B). After incubating the immunosensor with antigen and then Ab_2 or G-quadruplex bio-bar-coded AuNP-labeled Ab_2, the increasing electron-transfer resistance further decreased the ECL intensity (Figure 4B, curves b and d). However, the latter, in despite of the higher electron-transfer resistance, showed higher ECL intensity than HRP−Ab_2 double-coated AuNPs (Figure 3B, curves f and e; Figure 4B, curves d and c), indicating a different quenching mechanism from the steric hindrance.[28,29] Obviously, it resulted from the consumption of ECL coreactant in an enzymatic reduction.[30] Similarly, in the presence of hemin, the formed G-quadruplex/hemin bio-bar-code could show peroxidase-like activity, and the consumption of dissolve oxygen by the DNAzyme electrocatalyzed reduction led to a 4.8 times lower ECL intensity (Figure 4B, curves d and e) at a similar electron-transfer resistance.

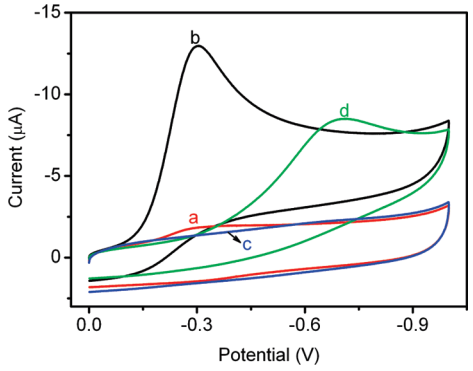

Figure 5. Cyclic voltammograms of Ab_1/chitosan/PDDA/CNT/GCE after incubation with 1 ng mL^{-1} AFP and then the Ab_2−bio-bar-coded AuNP−G-quadruplex/hemin probe (a, b) and HRP−Ab_2 double-codified AuNPs (c, d) in N_2-saturated (a, c) and air-saturated (b, d) 0.1 M pH 8.0 PBS containing 0.1 M KCl.

To further clarify the mechanism, the cyclic voltammograms of immunosensors after incubation with AFP and then Ab_2 labeled with the bio-bar-coded probe or HRP−Ab_2 double-codified

dx.doi.org/10.1021/ac200398x |*Anal. Chem.* 2011, 83, 5214–5221

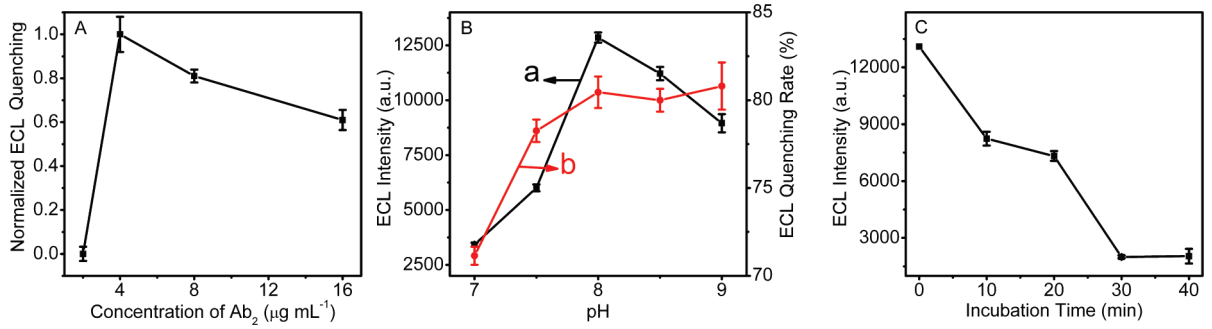

Figure 6. Effects of (A) Ab_2 concentration on the preparation of Ab_2−bio-bar-coded AuNP−G-quadruplex/hemin probe, (B) pH of detection solution using Ab_2−bio-bar-coded AuNPs in the absence (a) and presence (b) of hemin, and (C) incubation time on ECL response.

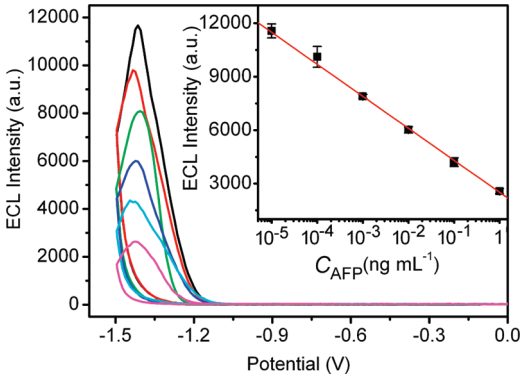

Figure 7. ECL−potential curves of immunosensor for AFP detection at 0.01, 0.1, 1, 10, and 100 pg mL^{-1} and 1 ng mL^{-1} in air-saturated 0.1 M pH 8.0 PBS containing 0.1 M KCl (from top to bottom). Inset: linear calibration for AFP detection.

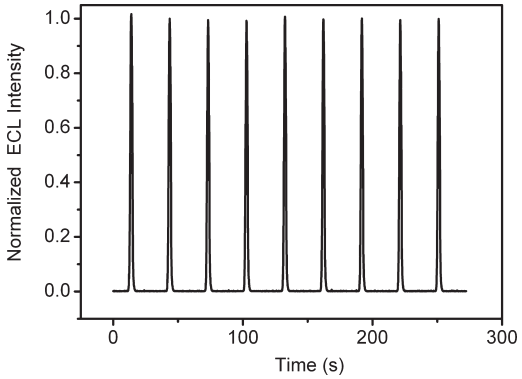

Figure 8. Continuous cyclic scans of ECL immunosensor for 1 ng mL^{-1} AFP in air-saturated pH 8.0 PBS containing 0.1 M KCl. Scan rate 0.1 V s^{-1}.

AuNPs were examined in the potential window of oxygen reduction (Figure 5). At the bio-bar-coded probe immobilized electrode, a well-defined reduction peak of dissolved oxygen occurred at −0.302 V (curve b), which was higher and much more positive than the reduction peak of −0.700 V that occurred at the HRP-immobilized electrode (curve d), indicating a stronger catalytic activity of the DNAzyme than HRP. Moreover, in the presence of hemin, a small peak could be observed at −0.297 V, which could be attributed to the electrochemical reduction of hemin. The reduced hemin then chemically reduced dissolved oxygen to OH^-. The electrode process could be described by the following mechanism:[35]

$$\text{Fe(III)DNAzyme} + e^- \rightarrow \text{Fe(II)DNAzyme} \quad (5)$$

$$4\text{Fe(II)DNAzyme} + O_2 + 2H_2O \rightarrow 4\text{Fe(III)DNAzyme} + 4OH^- \quad (6)$$

The DNAzyme-electrocatalyzed reduction of dissolved oxygen prohibited the formation of the excited state of QD by eqs 2 and 3, thus quenching the ECL emission. It should be pointed out that in the cathodic ECL process OH^- could be generated at close vicinity to electrode surface to shift the pH to higher values; however, the DNAzyme activity could be retained during the detection procedure possibly due to the distance of DNA−AuNPs as tags from electrode surface, where the buffer solution could buffer pH to an extent.

Optimization of Detection Conditions. Due to the intrinsic property of high surface-to-volume ratio, AuNPs could load numerous oligonucleotides with a relatively low content of Ab_2 by controlling the amount of Ab_2 to a certain concentration of AuNPs in the preparation step of Ab_2−AuNPs. As shown in Figure 6A, the bio-bar-coded probe showed the maximum ECL quenching when using 4 μg mL^{-1} Ab_2 for its preparation. The low content of Ab_2 lowered the binding ability of the bioconjugate in the sandwich-type immunoreaction, while high-content Ab_2 limited the loading of oligonucleotide on the nanoparticle surface, thus decreasing the quenching ability to the ECL emission. Thus, 4 μg mL^{-1} Ab_2 was used for the preparation of the bio-bar-coded probe.

The effect of detection solution pH on the ECL response of CdS QDs was shown in Figure 6B. In the examined pH range, the maximum ECL response of CdS QDs in the absence of hemin occurred at pH 8.0 (curve a). The ECL quenching rate increased with the increasing pH value and then reached a plateau at pH 8.0 (curve b). Taking into account the bioactivity of immunoreagents, a pH 8.0 PBS was selected as the detection solution.

At room temperature, the ECL quenching increased with the increasing incubation time used in sandwich-type immunoassay and then tended to a constant value after 30 min (Figure 6C), which showed a saturated binding between the analyte and the capture antibody on the immunosensor surface. Therefore, 30 min of incubation time was selected for the sandwich-type immunoassay.

Analytical Performance. Under the optimum conditions, the ECL intensity of the immunosensor decreased with the increasing

Table 1. Assay Results of Clinical Serum Samples Using the Proposed and Reference Methods

sample no.	1	1	1	1	2	3
proposed method (pg mL^{-1})	0.0199[a]	1.82[b]	19.8[c]	186[d]	2.85[b]	2.38[b]
reference method (ng mL^{-1})	2.09	2.09	2.09	2.09	2.78	2.24
relative error (%)	−4.78	−12.9	−5.26	−11.0	2.52	6.25

[a,b,c,d] The serum samples were diluted at 1×10^5, 1000, 100, and 10 times, respectively.

concentration of AFP in the incubation solution (Figure 7). The calibration plot showed a good linear relationship between the ECL intensity and the logarithm of the analyte concentration in the range from 0.01 pg mL^{-1} to 1 ng mL^{-1} with a correlation coefficient of 0.9987. The limit of detection (LOD) at a signal-to-noise ratio of 3 was 0.001 pg mL^{-1} (inset in Figure 7). This detection limit was not only much lower than those of previously reported QDs-based ECL immunoassay[28−30,36] but also at least 500 times lower than those reported by electrochemical immunoassay with different amplification strategies.[6,9,10] More importantly, this immunoassay method showed a wide detection range of 5 orders of magnitude and avoided the need of deoxygenation for electrochemical immunoassay.[6,9]

Reproducibility and Precision of Immunosensor. Both the intraassay and interassay precisions of the ECL immunosensor were examined five times at 0.1 ng mL^{-1} AFP. The relative standard deviations (RSD) were 2.5% and 5.6%, respectively, showing the good precision and acceptable fabrication reproducibility. Nine measurements of ECL emission upon continuous cyclic scans of the ECL immunosensor for 1 ng mL^{-1} AFP showed coincident signal with RSD of 0.73% (Figure 8), indicating acceptable reliability and stability of the detection signal.

Application in Detection of Serum Tumor Marker. The analytical reliability and application potential of the proposed method was evaluated by comparing the assay results of clinical serum samples using the proposed ECL immunosensor with the reference values obtained by commercial electrochemiluminescent single-analyte tests. When the level of serum tumor marker was over the calibration range, serum samples were appropriately diluted with 0.02 M pH 7.4 PBS prior to assay. The results listed in Table 1 show an acceptable agreement, with relative errors less than 12.9%, indicating the acceptable accuracy of the proposed method for the detection of AFP in clinical samples.

CONCLUSION

An ultrasensitive ECL immunoassay method has been developed by combining a newly designed bio-bar-coded nanoparticle probe with a CdS QDs-based immunosensor. The probe is prepared by the conjugation of hemin to a single-stranded guanine-rich oligonucleotide to form peroxidase-active G-quadruplex-based DNAzyme on Ab_2-attached AuNP surface. At the immunosensor the ECL intensity of QDs can be highly enhanced by PDDA-functionalized CNTs. The immunoassay follows an ECL quenching mechanism by coreactant consumption. The consumption of dissolved oxygen as coreactant results from the bio-bar-coded probe catalyzed electrochemical process. The ultrasensitivity comes from the enhanced ECL emission and high electrocatalytic efficiency of the bio-bar-coded probe. The immunoassay method shows a wide linear range and acceptable reproducibility, precision, and accuracy. It opens a new avenue for signal amplification of ECL immunosensing and extends the application field of QDs, DNAzyme, and bio-bar-coded technology.

AUTHOR INFORMATION

Corresponding Author

*Phone/fax: +86-25-83593593. E-mail: hxju@nju.edu.cn.

ACKNOWLEDGMENT

We gratefully acknowledge the National Basic Research Program of China (2010CB732400), the National Science Fund for Creative Research Groups (20821063), the projects (20875044, 21075055) from National Natural Science Foundation of China, and Natural Science Foundation of Jiangsu (BK2008014).

REFERENCES

(1) Wu, J.; Fu, Z. F.; Yan, F.; Ju, H. X. *TrAC-Trends Anal. Chem.* **2007**, *26*, 679–688.
(2) Ferrari, M. *Nat. Rev. Cancer* **2005**, *5*, 161–171.
(3) Stoeva, S. I.; Lee, J. S.; Smith, J. E.; Rosen, S. T.; Mirkin, C. A. *J. Am. Chem. Soc.* **2006**, *128*, 8378–8379.
(4) Wang, J.; Liu, G.; Jan, M. R. *J. Am. Chem. Soc.* **2004**, *126*, 3010–3011.
(5) Munge, B.; Liu, G.; Collins, G.; Wang, J. *Anal. Chem.* **2005**, *77*, 4662–4666.
(6) Tang, D.; Ren, J. *Anal. Chem.* **2008**, *80*, 8064–8070.
(7) Cui, R. J.; Liu, C.; Shen, J. M.; Gao, D.; Zhu, J. J.; Chen, H. Y. *Adv. Funct. Mater.* **2008**, *18*, 2197–2204.
(8) Wu, Y. F.; Chen, C. L.; Liu, S. Q. *Anal. Chem.* **2009**, *81*, 1600–1607.
(9) Mani, V.; Chikkaveeraiah, B. V.; Patel, V.; Gutkind, J. S.; Rusling, J. F. *ACS Nano* **2009**, *3*, 585–594.
(10) Lai, G. S.; Yan, F.; Ju, H. X. *Anal. Chem.* **2009**, *81*, 9730–9736.
(11) Shoji, E.; Freund, M. S. *J. Am. Chem. Soc.* **2001**, *123*, 3383–3384.
(12) Dai, Z. H.; Liu, S. H.; Bao, J. C.; Ju, H. X. *Chem.—Eur. J.* **2009**, *15*, 4321–4326.
(13) Chen, W. W.; Li, B. X.; Xu, C. L.; Wang, L. *Biosens. Bioelectron.* **2009**, *24*, 2534–2540.
(14) Zhao, W. A.; Ali, M. M.; Brook, M. A.; Li, Y. F. *Angew. Chem., Int. Ed.* **2008**, *47*, 6330–6337.
(15) Li, D.; Shlyahovsky, B.; Elbaz, J.; Willner, I. *J. Am. Chem. Soc.* **2007**, *129*, 5804–5805.
(16) Niazov, T.; Pavlov, V.; Xiao, Y.; Gill, R.; Willner, I. *Nano Lett.* **2004**, *4*, 1683–1687.
(17) Pelossof, G.; Tel-Vered, R.; Elbaz, J.; Willner, I. *Anal. Chem.* **2010**, *82*, 4396–4402.
(18) Nam, J. M.; Thaxton, C. S.; Mirkin, C. A. *Science* **2003**, *301*, 1884–1886.
(19) Zhu, D. B.; Tang, Y. B.; Xing, D.; Chen, W. R. *Anal. Chem.* **2008**, *80*, 3566–3571.
(20) Bi, S.; Yan, Y. M.; Yang, X. Y.; Zhang, S. S. *Chem.—Eur. J.* **2009**, *15*, 4704–4709.
(21) Hurst, S. J.; Lytton-Jean, A. K. R.; Mirkin, C. A. *Anal. Chem.* **2006**, *78*, 8313–8318.
(22) Pan, J.; Feng, S. S. *Biomaterials* **2009**, *30*, 1176–1183.
(23) Clarke, S.; Pinaud, F.; Beutel, O.; You, C.; Piehler, J.; Dahan, M. *Nano Lett.* **2010**, *10*, 2147–2154.
(24) Dong, H. F.; Gao, W. C.; Yan, F.; Ji, H. X.; Ju, H. X. *Anal. Chem.* **2010**, *82*, 5511–5517.

(25) Wu, X.; Liu, H.; Liu, J.; Haley, K. N.; Treadway, J. A.; Larson, J. P.; Ge, N.; Peale, F.; Bruchez, M. P. *Nat. Biotechnol.* **2003**, *21*, 41–46.
(26) Yin, Y. D.; Alivisatos, A. P. *Nature* **2005**, *437*, 664–670.
(27) Burda, C.; Chen, X. B.; Narayanan, R.; El-Sayed, M. A. *Chem. Rev.* **2005**, *105*, 1025.
(28) Jie, G. F.; Zhang, J.; Wang, D.; Cheng, C.; Chen, H. Y.; Zhu, J. J. *Anal. Chem.* **2008**, *80*, 4033–4039.
(29) Jie, G. F.; Liu, P.; Zhang, S. S. *Chem. Commun.* **2010**, *46*, 1323–1325.
(30) Liu, X.; Zhang, Y. Y.; Lei, J. P.; Xue, Y. D.; Cheng, L. X.; Ju, H. X. *Anal. Chem.* **2010**, *82*, 7351–7356.
(31) Ding, S. N.; Xu, J. J.; Chen, H. Y. *Chem. Commun.* **2006**, 3631–3633.
(32) Han, E.; Ding, L.; Jin, S.; Ju, H. X. *Biosens. Bioelectron.* **2011**, *26*, 2500–2505.
(33) Yu, W. W.; Qu, L.; Guo, W.; Peng, X. *Chem. Mater.* **2003**, *15*, 2854–2860.
(34) Wang, X. F.; Zhou, Y.; Xu, J. J.; Chen, H. Y. *Adv. Funct. Mater.* **2009**, *19*, 1444–1450.
(35) Zheng, N.; Zeng, Y.; Osborne, P. G.; Li, Y.; Chang, W.; Wang, Z. *J. Appl. Electrochem.* **2002**, *32*, 129–133.
(36) Jie, G. F.; Li, L. L.; Chen, C.; Xuan, J.; Zhu, J. J. *Biosens. Bioelectron.* **2009**, *24*, 3352–3358.